

The Ubiquitin Ligase CHIP/STUB1 Targets Mutant Keratins for Degradation

Stefanie Löffek,^{1*} Stefan Wöll,² Jörg Höhfeld,³ Rudolf E. Leube,² Cristina Has,⁴ Leena Bruckner-Tuderman,^{4,5} and Thomas M. Magin¹

¹Institute of Biochemistry and Molecular Biology, University of Bonn, Bonn, Germany; ²Institute of Molecular and Cellular Anatomy, RWTH Aachen University, Aachen, Germany; ³Institute of Cell biology, University of Bonn, Bonn, Germany; ⁴Department of Dermatology, University Medical Center Freiburg, Freiburg, Germany; ⁵Freiburg Institute of Advanced Studies, University of Freiburg, Freiburg, Germany

Communicated by Arnold Munnich

Received 23 October 2009; accepted revised manuscript 26 January 2010.

Published online 11 February 2010 in Wiley InterScience (www.interscience.wiley.com). DOI 10.1002/humu.21222

ABSTRACT: Keratin (K) intermediate filament proteins form cytoskeletal scaffolds in epithelia, the disruption of which leads to a large number of human disorders. *KRT5* or *KRT14* mutations cause epidermolysis bullosa simplex (EBS). The considerable intra- and interfamilial variability in EBS suggests modifying loci, most of which are unknown. In many human disorders, chaperones and the ubiquitin–proteasome system have been found to modify disease severity, thereby providing novel therapy targets. Here, we demonstrate upregulation of stress-induced Hsp70 and Hsp90 in two EBS models, namely, in neonatal *K5^{-/-}* mice and upon proteasome inhibition in cells that stably express the disease-causing mutation *K14-p.Arg125Cys*, both harboring keratin aggregates. Furthermore, proteasome inhibition caused nuclear translocation of pHSF-1 and an increase in *K14-p.Arg125Cys*-positive aggregates in cells. Overexpression of the chaperone-associated ubiquitin ligase CHIP/STUB1 strongly reduced keratin aggregates through increased degradation of mutant *K14*. Using CHIP-p.Met1Ala142del (ATPR-CHIP), we demonstrated the involvement of Hsc70 and Hsp70 in mutant keratin degradation. Our data uncover common principles between EBS and other protein misfolding disorders, revealing that aggregation-prone keratins are targeted by components of the chaperone machinery. Thus, modulation of the chaperone machinery using small molecules may represent a novel therapeutic strategy for dominant EBS, allowing reformation of an intact keratin cytoskeleton. *Hum Mutat* 31:466–476, 2010. © 2010 Wiley-Liss, Inc.

KEY WORDS: epidermolysis bullosa simplex; EBS; *KRT5*; *KRT14*; Hsp70; Hsc70; CHIP

Introduction

Keratins K5 and K14 are the major keratins in the basal keratinocytes of stratified epithelia where they form the intermediate

filament (IF) cytoskeleton. They are members of a large family with 54 known genes, grouped into 28 type I and 26 type II IF genes [Schweizer et al., 2006]. Like all other keratins, the type I K14 and the type II K5 proteins heterodimerize and subsequently polymerize into 10- to 12-nm wide IF. These associate with plakin and plakophilin family members to form a supracellular scaffold that protects the epidermis against mechanical and other forms of stress [Coulombe et al., 2009; Fuchs and Cleveland, 1998; Omary et al., 2004]. Mutations in *KRT5* (MIM# 148040) and *KRT14* (MIM# 148066) weaken the integrity of the keratin cytoskeleton and eventually result in the aggregation of the keratin cytoskeleton and cause intracellular cytolysis, a phenotype leading to the skin disorder epidermolysis bullosa simplex (EBS). EBS is a rare inherited skin disorder arising from minor mechanical trauma [Coulombe et al., 2009]. Most cases of EBS result from dominantly acting mutations in keratins *KRT5* and *KRT14*, which in rare cases, for example, the herpetiform Dowling-Meara subtype of EBS (EBS-DM) can be life-threatening [Fine et al., 2008]. Currently, it is well accepted that intracellular and intraepidermal cytolysis, due to a compromised cytoskeleton is the primary cause for EBS [Fuchs and Cleveland, 1998]. More recently, an increase in proinflammatory cytokines and chemokines, which mediate an immune response, and an increased number of Langerhans cells were found to contribute to the pathology of EBS [Lu et al., 2007; Roth et al., 2009]. The potential contribution of aggregated keratins, which might cause a stress response, has so far not been examined.

The presence of protein aggregates in EBS skin is reminiscent of those found in protein-conformational disorders, like Alzheimer (AD) and Parkinson disease (PD) [Muchowski and Wacker, 2005], and it has been proposed that keratin disorders are also protein folding disorders [Chamcheu et al., 2009; Lee et al., 2008]. Due to the presence of ubiquitin, components of the proteasome complex and molecular chaperones, including Hsp70 (see HSPA1A; MIM# 140550) and Hsp40 (see DNAJB1; MIM# 604572) in those aggregates [McClellan et al., 2005; Muchowski and Wacker, 2005], it is widely accepted that protein-conformational disorders result from a failure of the protein quality control. With regard to potential therapy approaches of EBS it is worth noting that overexpression of intact keratins in transgenic mice can restore tissue homeostasis [Hesse et al., 2007; Zhou et al., 2003].

Most remarkably, in contrast to aggregates found in neurodegenerative disorders keratin aggregates are not static but dynamic assemblies that turn over with $t_{1/2}$ of ~12 min [Werner et al., 2004]. This suggests that keratin assembly may be a regulated process and raises the question whether chaperones, for example, Hsc70 (HSPA8; MIM# 600816), Hsp70 (Hsc/p70), or Hsp90 (see HSP90AA1; MIM#

Additional Supporting Information may be found in the online version of this article.

*Correspondence to: Stefanie Löffek, Institute of Biochemistry and Molecular Biology, University of Bonn, Nussallee 11, 53115 Bonn, Germany.

E-mail: loeffek@ibmb.uni-bonn.de

140571) are involved in this process as it has been demonstrated for p38 MAPK as a keratin modulator [Woll et al., 2007].

The activity of the stress-induced Hsp70 and its constitutively expressed cognate Hsc70 is regulated by a family of >40 cochaperones that provide substrate specificity and assist in substrate recruitment to Hsc/p70, as well as nucleotide exchange factors that regulate the ATPase cycle. Although the majority of cochaperones serve the refolding of proteins into the native state, cochaperones, like CHIP (carboxyl terminus of Hsc/p70 interacting protein; approved symbol *STUB1*; MIM# 607207) can also redirect Hsc/p70 to the ubiquitin-proteasome system responsible for the degradation of misfolded proteins [Esser et al., 2004]. Strong evidence for the involvement of cochaperones in keratin assembly stems from the genetic characterization of the cochaperone Mrj (also known as Dnajb6) that regulates Hsc/p70 activity in the mammalian cytoplasm. In Mrj-deficient mice, the organization of K8, K18, and K19 is strongly affected. Instead of forming a normal cytoskeleton, they accumulate into cytoplasmic aggregates, which morphologically resemble those found in epidermal keratinopathies [Watson et al., 2007], indicating an involvement of the cochaperone in keratin assembly. Therefore, approaches that moderate the soluble state of keratins might allow the chaperone system to become active. However, the presence of ubiquitin in both neurodegenerative disorders and cytoplasmic inclusions of mutant keratins, for example, the so-called Mallory bodies, imply the ubiquitin-proteasome pathway (UPP) as a regulator of mutant keratin turnover [Schulz, 2008; Zatloukal et al., 2007]. This pathway involves the sorting of Hsc/p70 substrate proteins from a chaperone-bound state to the proteasome, which is triggered by the chaperone-associated E3 ubiquitin ligase CHIP.

Here, we investigated whether a modulation of the Hsc/p70 chaperone machinery might affect the aggregation of mutant K14 in an EBS cell culture model. Proteasome inhibition caused nuclear translocation of pHSF-1, eventually leading to an upregulation of stress-induced Hsp70 and Hsp90 and by a strong increase in K14-p.Arg125Cys-positive aggregates. Overexpression of the ubiquitin ligase CHIP strongly reduced keratin aggregates through increased degradation of mutant K14 in an Hsc/p70-dependent mechanism. Therefore, the regulated interplay between the Hsc/p70 chaperone machinery and the ubiquitin/proteasome system appears to control the fate of mutant keratins. Our data uncover common principles between EBS and other protein misfolding disorders, revealing that aggregation-prone keratins are targeted by components of the chaperone machinery.

Materials and Methods

DNA Cloning

The mOrange-tagged CHIP construct was created by cloning the mOrange-CHIP (CHIP cDNA sequence NM_005861) fragment into the NotI/SalI site of pLNCX2 (Invitrogen, Carlsbad, CA). pCW-7 for expression of His-tagged ubiquitin was obtained from ATCC (Rockville, MD) [Ward et al., 1995]. For CHIP-p.Met1_Ala142del (Δ TPR-CHIP) expression, a pcDNA3.1 Δ TPR-CHIP-myc-His construct was utilized [Ballinger et al., 1999].

Cell Culture and Transient Transfection

MCF-7 human breast cancer cells stably expressing eYFP-K14-p.Arg125Cys were described before [Werner et al., 2004]. MCF-7 eYFP-K14-p.Arg125Cys cells were plated 24 hr prior to transfection and grown to 80% confluency. Cells were transfected with

DNA constructs using lipofectamine 2000 according to the manufacturer's protocol.

Human primary keratinocytes were obtained by trypsinization of control and the EBS skin biopsies and cultured in serum-free, low-calcium keratinocyte growth medium supplemented with bovine pituitary extract and epidermal growth factor (KGM; Invitrogen, Karlsruhe, Germany) for two to six passages as described [Konig et al., 1992]. The following mutants were used: K14 p.Leu143Pro, K14-p.Arg125Cys, and K14 p.Tyr415His.

Inhibition of the Proteasome and Hsc/p70

Proteasome inhibitors MG132 (42 mM), Epoxomicin (Epox) (1 mM), ALLN (N-acetyl-Leu-Leu-norleucinal) (26 mM), and the small molecule KNK437 (KNK, 3,4-Methylenedioxy-benzylidene- γ -butyrolactam) (5 mg/mL) were obtained from Calbiochem (LaJolla CA), solubilized in DMSO, and applied in the indicated concentrations.

Proteasome Inhibition

To determine proteasome inhibition, the fluorogenic Suc-Leu-Leu-Val-Tyr-AMC peptide (Suc-LLVT-AMC) was used as substrate. MCF-7 cells were cultured in 24-well plates in DMEM medium containing 10% FBS for 24 hr. Cells were pretreated with different proteasome inhibitors for 3 hr in the indicated concentrations. Then, medium containing Suc-LLVT-AMC and the corresponding proteasome inhibitor was added. Fluorescence was recorded at 10-min intervals for 2 hr at excitation 360 ± 20 nm and emission 460 ± 20 nm using a Multi-Detection microplate Reader.

Immunofluorescence Microscopy

MCF-7 eYFP-K14-p.Arg125Cys cells grown on coverslips were fixed in methanol for 3 min, followed by acetone fixation for 30 sec. Fixed cells were incubated in 1% BSA/TBS containing the specific antibodies Ks 8.7 against K8, anti- α -tubulin (NeoMarkers, Fremont, CA), anti-pHSF-1 (Santa Cruz, Santa Cruz, CA), His₆ (clone 2; Roche, Indianapolis, IN), 9E10 against myc, and K14 antiserum (Magin Lab) for 1 hr at room temperature. After repetitive washing in TBS cells were incubated in Cy3-conjugated goat antirabbit or antimouse antibodies, washed again, and mounted in ProLong Gold antifade reagent (Invitrogen). Negative controls were performed by omission of primary antibodies.

Sections were examined with a photomicroscope (Axiophot 2E; Carl Zeiss, Germany) equipped with Zeiss Plan-Neofluar and Aplanachrom lenses $63 \times$, NA 1.25 and 1.4, and recorded with a digital camera (AxiocamHR, Carl Zeiss, Germany). Image analysis and processing were performed using the AxioVision LE 4.6 (Carl Zeiss) and Adobe Illustrator Artwork CS4 software. Confocal images were recorded on a LSM710 microscope (Carl Zeiss; equipped with the same lenses). For colocalization, Z stacks (10 consecutive sections, distance $0.49 \mu\text{m}$) were obtained using the LSM710 (Zeiss) microscope. The original image was further processed by ZEN Version 5.0 software to determine pixel counts and colocalization data. All pixels above the set threshold values were counted and exported to an image showing only the colocalized pixels (maximum intensity projection). Minimum threshold intensity was set based on nonspecific signal intensity for every color.

Live-Cell Imaging

Recording of fluorescence patterns on an inverse confocal fluorescence microscope (SP5, Leica, Allendale, NJ) were

performed as described previously [Windoffer et al., 2006; Windoffer and Leube, 2004].

as means \pm SE of three independent experiments and representative immunoblots are shown.

Western Blotting and IF-Enriched Cytoskeletal Extract Preparation

Total protein lysates were obtained by solubilizing MCF-7 cells in $5 \times$ Laemmli sample buffer.

IF-enriched cytoskeletal extracts were prepared by cytolysis of confluent cell cultures with ice-cold low-salt buffer (10 mM Tris-HCl, pH. 7.6, 140 mM NaCl, 5 mM EDTA, 5 mM EGTA, 0.5% Triton X-100, 2 mM phenylmethylsulfonyl fluoride), a subsequent centrifugation step to separate the Triton X-100-soluble cytoskeletal fraction from the Triton X-100-insoluble cytoskeletal fraction, which was then resuspended in ice-cold high-salt buffer (10 mM Tris-HCl, pH. 7.6, 140 mM NaCl, 1.5 M KCl, 5 mM EDTA, 5 mM EGTA, 1% Triton X-100, 2 mM phenylmethylsulfonyl fluoride), homogenized, pelleted by centrifugation, and solubilized in $5 \times$ Laemmli sample buffer.

Samples were separated on 10% SDS-PAGE under reducing conditions and transferred to nitrocellulose membranes. Blots were incubated with the following antibodies: anti-CHIP (Santa Cruz), anti-Hsp90 (Santa Cruz), P4G7 against Ubiquitin (Abcam, Cambridge, MA), N27F3-4 against Hsp/c70 (Stressgen, Ann Arbor, MI), gp11 against K8 and K18 (Progen, Germany), anti-GFP and K14 antiserum (Magain Lab). Membranes were washed three times for 5 min in 0.05% Tween/TBS and incubated with secondary antibodies (goat antirabbit, goat antiguinea pig, and antimouse sera) conjugated to horseradish peroxidase (1:40,000 dilution, Dianova, Hamburg, Germany) for 1 hr at room temperature. After three washes with 0.05% Tween/TBS solution, immunoreactive proteins were detected using the ECL Western blotting detection reagents. Immunoblots were quantified by determining the signal intensities using ImageJ (National Institutes of Health, <http://rsb.info.nih.gov/ij/>). Data are presented

Purification of His-Tagged Ubiquitin

His-tagged ubiquitin transfected MCF-7 eYFP-K14-p.Arg125Cys cells were solubilized in denaturation buffer (50 mM NaH_2PO_4 , 300 mM NaCl, 8 M urea) and cell lysate was applied to a Protino Ni-TED/IDA column (Macherey-Nagel, Germany). His-Ubiquitin was eluted in elution buffer (20 mM NaH_2PO_4 , 500 mM NaCl, 500 mM Imidazol, 8 M urea), eluate was precipitated by TCA and precipitate was solubilized in $5 \times$ Laemmli sample buffer.

Results

The Expression of Chaperones is Induced in Different EBS Models

A large number of dominant mutations in *KRT5* and *KRT14*, genes cause EBS by affecting the organization of the cytoskeleton, adhesion, and migration of keratinocytes and results in the formation of keratin aggregates. The notion that aggregates containing mutant keratins are dynamic in a cell culture model suggests that aggregation may be a reversible process, and raises the question of whether chaperones and the ubiquitin proteasome system are involved [Werner et al., 2004]. This prompted us to examine chaperone expression in *K5^{-/-}* mice, a mouse model for EBS that displays extensive K14 aggregates [Peters et al., 2001]. Microarray analysis revealed a fourfold increase of stress-induced Hsp70 mRNA in neonatal *K5^{-/-}* mice compared to wild-type controls (for complete expression profiling array see: <http://www.ncbi.nlm.nih.gov/geo/query/acc.cgi?acc=GSE7663>). Furthermore, in the absence of K5, Hsp90 and the stress-induced Hsp70 protein (71 kDa) were elevated while the expression of Hsc70 was unchanged (Fig. 1A).

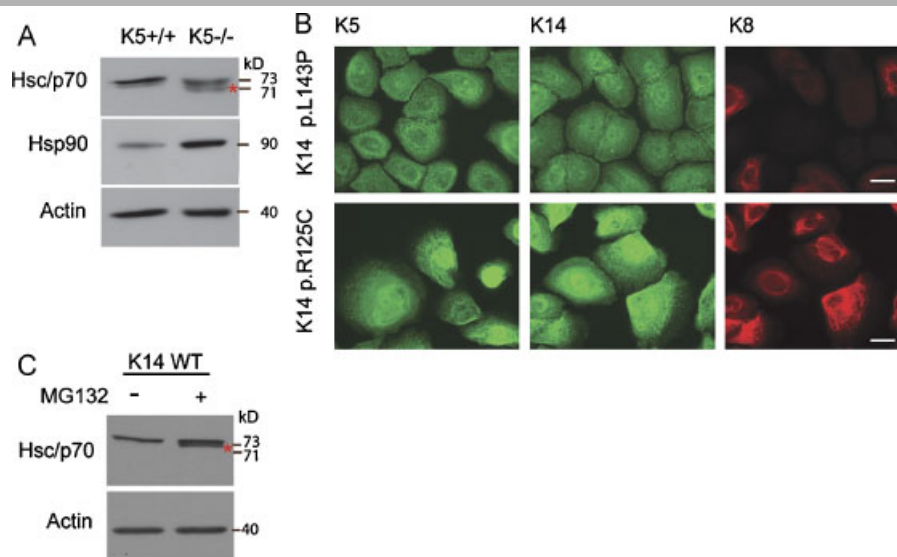


Figure 1. HSP expression in mouse and human EBS model systems. **A:** Skin samples from neonatal *K5^{-/-}* and wild-type mice were prepared as described before [Roth et al., 2009]. A total of 100 μ g of total lysate was separated by 10% SDS-PAGE, transferred to nitrocellulose, and immunoblotted with anti-Hsc/p70 and Hsp90 antibodies. Actin staining was used as loading control. *Indicates stress-induced 71-kDa Hsp70. **B:** Primary human keratinocytes (upper panel: K5 WT/K14 p.Leu143Pro [K14-p.L143P]; lower panel: K5 WT/K14-p.Arg125Cys [K14-p.R125C]) were fixed and stained with K5, K14, and K8 antibodies. Scale bar, 10 μ m. **C:** Total lysates of wild-type primary keratinocytes were cultured in the presence and in the absence of MG132 (100 μ M) for 6 hr. Equal amounts of cell extracts were analyzed by Western blotting with Hsc/p70 and actin antibodies. *Indicates stress-induced 71-kDa Hsp70.

We then isolated primary keratinocytes from different EBS patients. Keratinocytes expressing a mild mutation of EBS-DM (like the K14 mutants p.Leu143Pro and p.Tyr415His [not shown]) showed no alteration of K5, K14, and K8 filaments (Fig. 1B, upper panel). In contrast, a mutation that causes severe keratin misfolding, for example, K14-p.Arg125Cys showed clusters of keratin aggregates and ring-like structures in the cell periphery under normal cell culture conditions (Fig. 1B, lower panel), in line with previous reports [Kitajima et al., 1989; Russell et al., 2004]. Inhibition of the proteasome, by using the proteasome inhibitor MG132, revealed an induction of stress-induced Hsp70 in primary wildtype keratinocytes (Fig. 1C); however, the response to proteasome inhibition in the different K14 mutants was very variable (data not shown). As the EBS patient-derived primary cells were derived from different individual genotypes there is the possibility that the differences observed in these cells is a consequence of background and passage number variations. To analyze the effect of modulated chaperone/cochaperone expression, we therefore turned to a well-established cell culture system in which we had stably transfected the EBS causing mutation K14-p.Arg125Cys in MCF-7 cells [Werner et al., 2004]. To elevate the expression of chaperone transcription via pHSF-1 activation, we first applied stress by blocking proteasome activity by different proteasome inhibitors (MG132, ALLN, and the irreversible inhibitor Epoxomicin). An *in vivo* proteasome assay revealed efficient inhibition of the proteasome upon treatment with all three proteasome inhibitors in cultured cells (Fig. 2A). This was accompanied by a dose-dependent accumulation of ubiquitinated proteins in total cell lysates (Fig. 2B) and by nuclear translocation of the transcription factor pHSF-1 (Fig. 2D). As expected, Western blotting of total protein extracts showed an induction of the stress-induced Hsp70 protein upon proteasome inhibition indicated by the appearance of the 71-kDa band, whereas the constitutively expressed Hsc70 (73 kDa) was unchanged. However, the protein levels of the E3 ubiquitin ligase CHIP were unaltered. In addition, we detected an accumulation of mutant K14 and the endogenous K8/K18 (Fig. 2C), indicating that keratin degradation is mediated via the proteasome pathway, in line with previous reports [Jaitovich et al., 2008; Ku and Omary, 2000].

Video and high-resolution confocal microscopy (Fig. 3A and B and Supp. Movie S1) revealed a time-dependent movement of keratin aggregates toward a juxtanuclear position, accompanied by a reduction of remaining filamentous K14 in the presence of the proteasome inhibitor MG132. In addition, the number of aggregates increased throughout the cytoplasm following MG132 treatment in a time-dependent manner (quantification in Fig. 3A), indicating the dynamic nature of keratin aggregates. Application of ALLN (data not shown) and the irreversible inhibitor Epoxomicin caused the same phenotype (Supp. Movie S2). Proteasome inhibition by MG132 neither affected microtubules nor actin (Fig. 3C and D) at least at the level of immunofluorescence microscopy, supposing that keratin aggregates resulted from impaired degradation of keratins [Helfand et al., 2004; Liovic et al., 2003; Werner et al., 2004; Woll et al., 2005].

CHIP Overexpression reduces K14-p.Arg125Cys-Positive Aggregates

Recently, we detected a direct interaction between Hsp/c70 with the K5 head domain [Planko et al., 2007]. In support, confocal microscopy corroborated a colocalization between K14 and endogenous Hsc/p70 in MCF-7 (Fig. 4B). To ascertain whether the Hsc/p70-associated ubiquitin ligase CHIP had any impact on

mutant keratin aggregates, two different CHIP cDNA constructs were transfected into K14-p.Arg125Cys expressing cells. Whereas the Flag-tagged CHIP construct was exclusively used for biochemical analysis, the mOrange-tagged CHIP was used for both biochemical analysis and direct immunofluorescence.

The number of total cells containing keratin aggregates was reduced by 25–40% compared to mock transfectants as judged by immunofluorescence (Fig. 5A). From those cells that overexpress CHIP, only about 18% show K14-p.Arg125Cys aggregates in the cell periphery (quantification in Fig. 4C). Taking together the data reveal a central role of CHIP in keratin quality control as a facilitator of mutant keratin turnover.

To verify directly whether CHIP triggers keratin degradation, Triton X-100-soluble and insoluble fractions were analyzed by Western blotting (Fig. 5D). The amount of K14 in total cell lysates was reduced by about 20% in cells overexpressing CHIP (transfection efficiency about 45%) compared to mock control, strongly supporting proteasomal degradation of mutant K14 (Fig. 5D). Unexpectedly, the Triton X-100-soluble fraction containing K14-p.Arg125Cys was unaffected, whereas the Triton X-100-insoluble fraction, representing both keratin aggregates and remaining IF containing low amounts of K14, was preferentially degraded in CHIP-expressing cells. Given that K14 is incorporated into the endogenous keratin IF formed by K8, K18, and K19 [Werner et al., 2004], this raised the question whether CHIP also acted on the endogenous type II K8. We found a 10% reduction of K8 in the Triton X-100-insoluble fraction (Fig. 5C). In line with its causative effect on keratin aggregation, we suggest that the presence of the p.Arg125Cys mutation renders it an excellent CHIP substrate. Furthermore, the minor effect of CHIP on K8 compared to K14-p.Arg125Cys may result from the greater stability of K8/K18 complexes, as suggested in another study [Ku and Omary, 2000].

Mutant K14 is Ubiquitinated In Vivo

The observation that the ubiquitin ligase CHIP promotes degradation of keratins infers their ubiquitination. Previously, monoubiquitination of single, overexpressed keratins K8 or K18 in the presence of the proteasome inhibitor ALLN was reported [Ku and Omary, 2000]. Following expression of His-tagged ubiquitin in K14-p.Arg125His cells, we detected high-molecular weight forms of K14 representing polyubiquitinated species (Fig. 6A). To confirm K14 ubiquitination, His-tagged ubiquitin was enriched by affinity chromatography. In addition to large amounts of ubiquitinated cellular proteins, ubiquitinated K14 species were identified by Western blotting (Fig. 6B). To relate this to aggregated keratins, His-ubiquitin transfected eYFP-K14-p.Arg125Cys cells were stained against ubiquitin and analyzed by confocal microscopy (Fig. 6C, left panel shows one optical section of a Z stack). Following image analysis, colocalized pixels (right panel, maximum intensity projection) of ubiquitin and the mutant K14 were identified. Thus, aggregated keratins are ubiquitinated in a cell culture model of EBS. This was in line with the reported ubiquitination of mutant K14-p.Arg125Cys and the absence of ubiquitin on wildtype K14 [Yoneda et al., 2004].

CHIP-Mediated Degradation of Mutant Keratins Depends on Hsc/p70

CHIP and Hsc/p70 interact with each other via the N-terminal TPR domain in CHIP and the C-terminal EEVD motif of Hsc/p70 [Arndt et al., 2007; Esser et al., 2004]. However, there is increasing

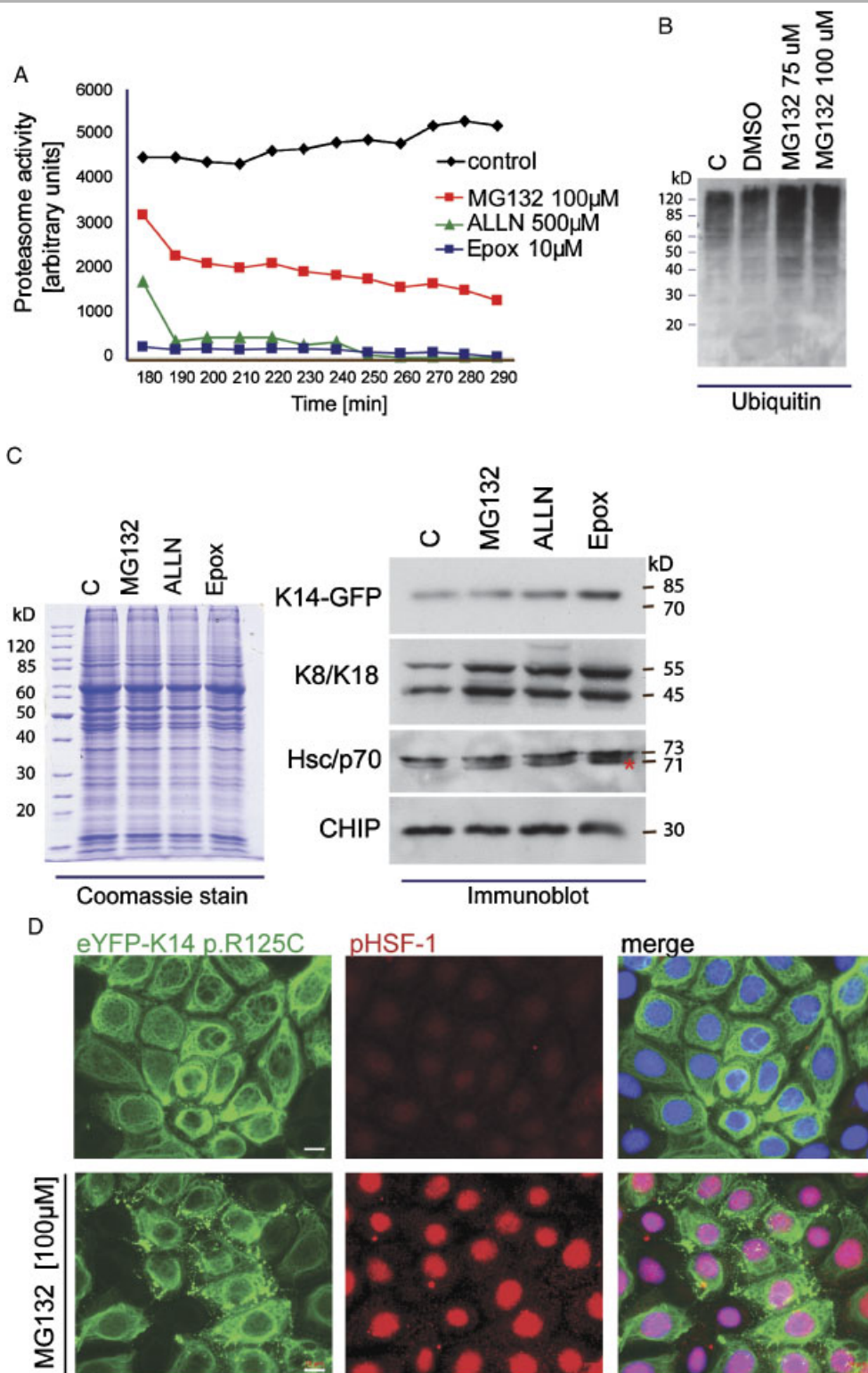


Figure 2. Induction of HSP expression by proteasome inhibition. **A:** In vivo proteasome activity was measured using the fluorogenic peptide Suc-Leu-Leu-Val-Tyr-AMC. The assay was performed as described in Materials and Methods. Proteasome inhibitors were used in the indicated concentrations. **B:** MCF-7 cells stably expressing eYFP-K14-p.Arg125Cys were grown in the presence of increasing concentrations of MG132 for 6 hr. Equal amounts of cell extracts were analyzed by Western blotting with ubiquitin antibody. **C:** MCF-7 cells stably expressing eYFP-K14-p.Arg125Cys were grown in the absence and presence of MG132 (100 μM), ALLN (500 μM), and Epoxomicin (10 μM) for 6 hr. Equal amounts of protein, shown by Coomassie staining, were detected by Western blotting with GFP (to detect mutant K14 fused to eYFP), K8/K18, Hsc/p70, and CHIP antibodies. **D:** MCF-7 cells stably expressing eYFP-K14-p.Arg125Cys (K14-p.R125C) were grown in the absence and presence of MG132 (100 μM) for 6 hr, fixed, and stained with pHSF-1 antibody. The keratin cytoskeleton is depicted by eYFP autofluorescence. Note increased aggregate numbers and induction of pHSF-1 following MG132 treatment (middle and right panel, merged image). Scale bar, 10 μm.

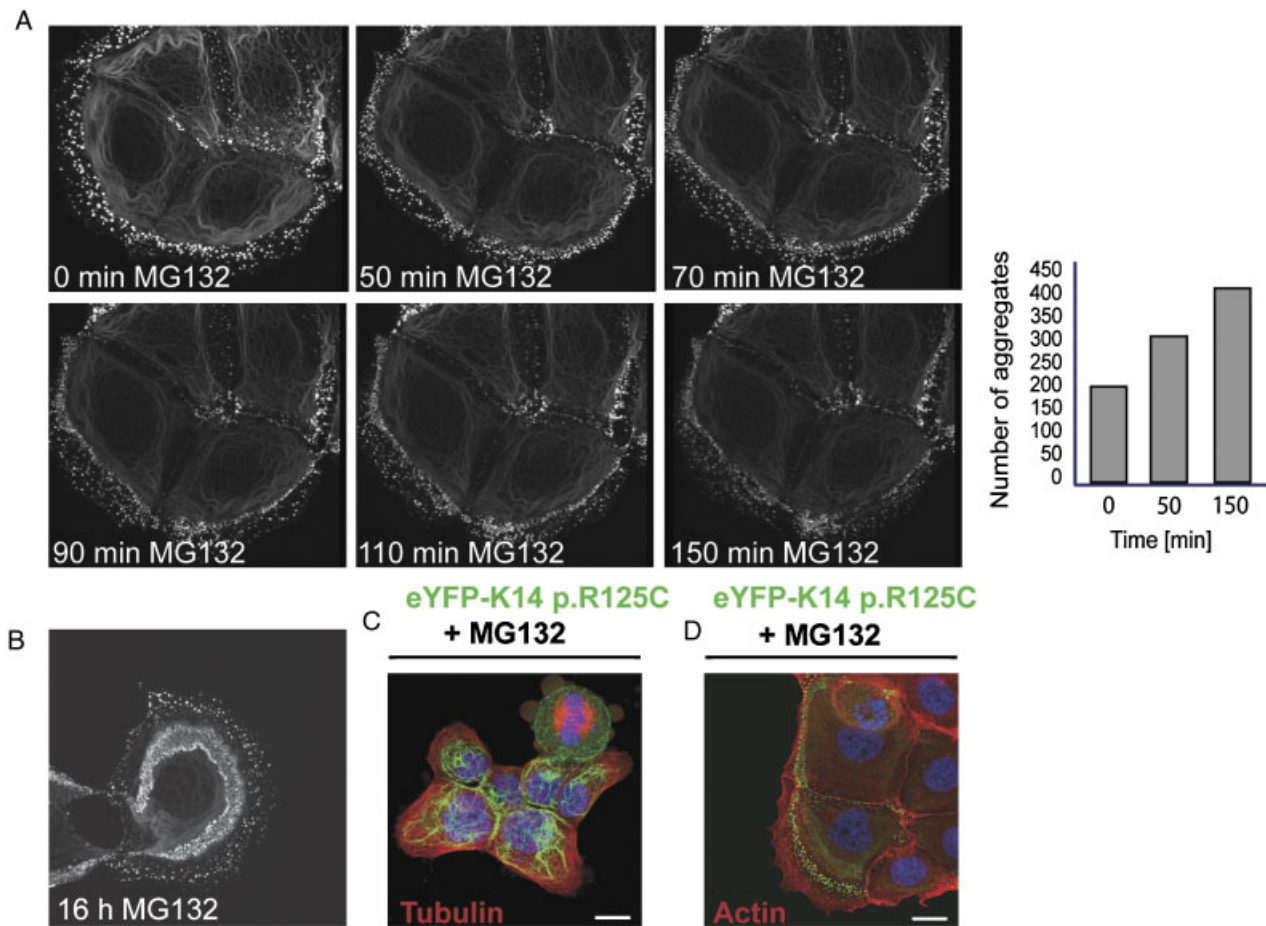


Figure 3. Enhanced keratin aggregate formation is mediated by the inhibition of the proteasome. **A:** Fluorescence images of a time-lapse recording (from Supp. Movie S1) showing time-dependent increase in eYFP-K14-p.Arg125Cys aggregates at different time points. Graph, quantitative display of aggregates. **B:** Fluorescence images of MCF-7 eYFP-K14-p.Arg125Cys [K14-p.R125C] cells following 16-hr treatment with MG132. **C:** eYFP-K14-p.Arg125Cys-transfected MCF-7 (K14-p.R125C) cells treated with MG132 for 6 hr, fixed, and stained with tubulin antibody and phalloidin to detect actin. Scale bar, 10 μ m.

evidence that CHIP possesses chaperone activity that can lead to the refolding of stress-damaged proteins in an Hsc/p70-independent manner [Rosser et al., 2007; Tetzlaff et al., 2008]. Besides its ubiquitin ligase activity, CHIP is also involved in the regulation of the activity of the transcription factor HSF-1 and stimulates the expression of HSF-1-controlled genes [Dai et al., 2003]. Consistent with this, elevation of CHIP levels upon transient transfection led to a 70% increase in the protein levels of stress-induced Hsp70 (Fig. 4A). The pronounced effects of CHIP expression on keratin aggregation may thus reflect the increased formation of an Hsc/p70-CHIP chaperone complex that targets keratins for proteasomal degradation.

To assess whether degradation of mutant keratins by CHIP indeed involves an interaction with Hsc/p70, either full-length CHIP or CHIP-p.Met1_Ala142del (Δ TPR-CHIP) mutant was transiently transfected. In the presence of wild-type CHIP, ~20% of the cells contained peripheral aggregates, whereas in Δ TPR-CHIP-overexpressing cells, 72% contained K14-positive aggregates (quantification in Fig. 4C). This supports a functional interaction of CHIP with Hsc/p70 during the degradation of keratins. Biochemical analysis revealed an increase in the Triton X-100-insoluble fraction in cells overexpressing Δ TPR-CHIP compared to the ~20% decrease in cells with wild-type CHIP (Fig. 4D). The minor effect of Δ TPR-CHIP might be due to

induction of the endogenous CHIP in those transfectants (Fig. 4D, right panel). The inhibition of the constitutively expressed Hsc70 of the transcription level, by the small molecule KNK437 (Fig. 4E) in K14 mutant cells led to a strong reduction of the soluble K14 pool but had no effect on the Triton X-100-insoluble pool, confirming the importance of CHIP-Hsc/p70 interaction. Based on the direct interaction between K5 and Hsc70 [Planko et al., 2007] and between K14 and Hsp70 [Setty and Magin, unpublished], we infer a mechanism in which binding of CHIP to keratins is mediated via Hsc/p70.

Discussion

Severe EBS results from dominantly acting *KRT5* and *KRT14* mutations, leading to the formation of cytoplasmic protein aggregates and fragile keratinocytes. Such protein aggregates closely resemble those found in vimentin-induced cataracts, in chronic liver disorders, AD, PD, and several other neurodegenerative disorders [Auluck and Bonini, 2002; Auluck et al., 2002; Bornheim et al., 2008; Strnad et al., 2008]. Here, we demonstrate for the first time that the stress-induced Hsp70 and Hsp90 were upregulated in neonatal *K5*^{-/-} mice and, upon proteasome inhibition, in a cell culture model of EBS at the RNA and protein level. In line with recent reports, this supports the view that EBS

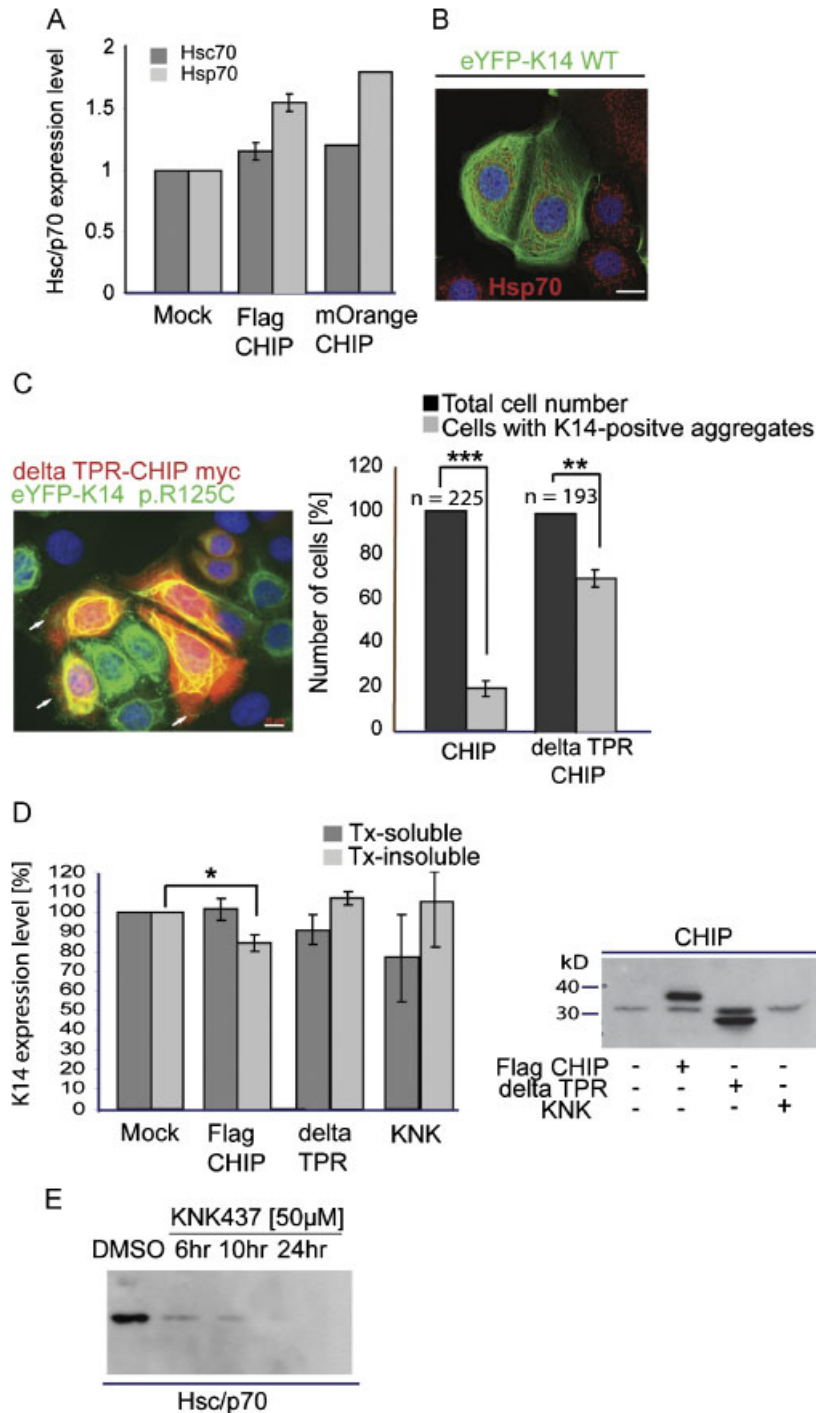


Figure 4. CHIP-mediated degradation of mutant keratin depends on Hsc/p70. **A:** Cells were transiently transfected with empty vector (mock) and either Flag-tagged or mOrange-tagged CHIP. After 24 hr, total cells were lysed, separated on 10% SDS-PAGE, and immunoblotted with Hsc/p70 antibodies (not shown). Graph shows quantification of two independent experiments. **B:** MCF-7 cells were transiently transfected with wild-type K14, fixed, and stained with Hsc/p70 antibodies. Note the colocalization of Hsc/p70 and wild-type K14. **C:** Cells were transiently transfected with either mOrange-tagged CHIP or CHIP Δ TPR-myc-His. After 24 hr, transfected cells were fixed and stained with DAPI. Autofluorescence of eYFP-K14-p.Arg125Cys (K14-p.R125C) and anti-myc staining (CHIP Δ TPR-myc-His) is shown. Scale bar, 10 μ m. Quantification of CHIP or CHIP-p.Met1_Ala142del-expressing cells (Δ TPR-CHIP) containing K14-positive aggregates is shown. *** $P = 2 \times 10^{-6}$, ** $P = 7 \times 10^{-5}$. **D:** Cells were transiently transfected with empty vector (mock) and either Flag-tagged CHIP or Δ TPR-CHIP-myc-His. In addition, cells were grown in the presence of the Hsc/p70 inhibitor 3,4-Methylenedioxy-benzylidene- γ -butyrolactam (KNK437, in a final concentration of 50 μ M). After 24 hr, cell lysates were fractionated into Tx-soluble and Tx-insoluble pool. Two percent of each fraction was separated by 10% SDS-PAGE, and immunoblotted with CHIP antibodies. Quantification shows signal intensity of K14 immunoblots (Tx-soluble and Tx-insoluble fraction, not shown). Immunoblot (right panel) shows CHIP expression level in total cell lysate. * $P = 0.002$. **E:** MCF-7 wild-type cells were grown in the absence (DMSO) or in the presence of the Hsc/p70 inhibitor 3,4-Methylenedioxy-benzylidene- γ -butyrolactam (KNK437) in a final concentration of 50 μ M for indicated time points. Cells were lysed, equal amounts of protein were separated by 10% SDS-PAGE, and immunoblotted with Hsc/p70 antibodies. Data are presented as means \pm SE of three independent experiments. The P values were calculated using the Student's t -test.

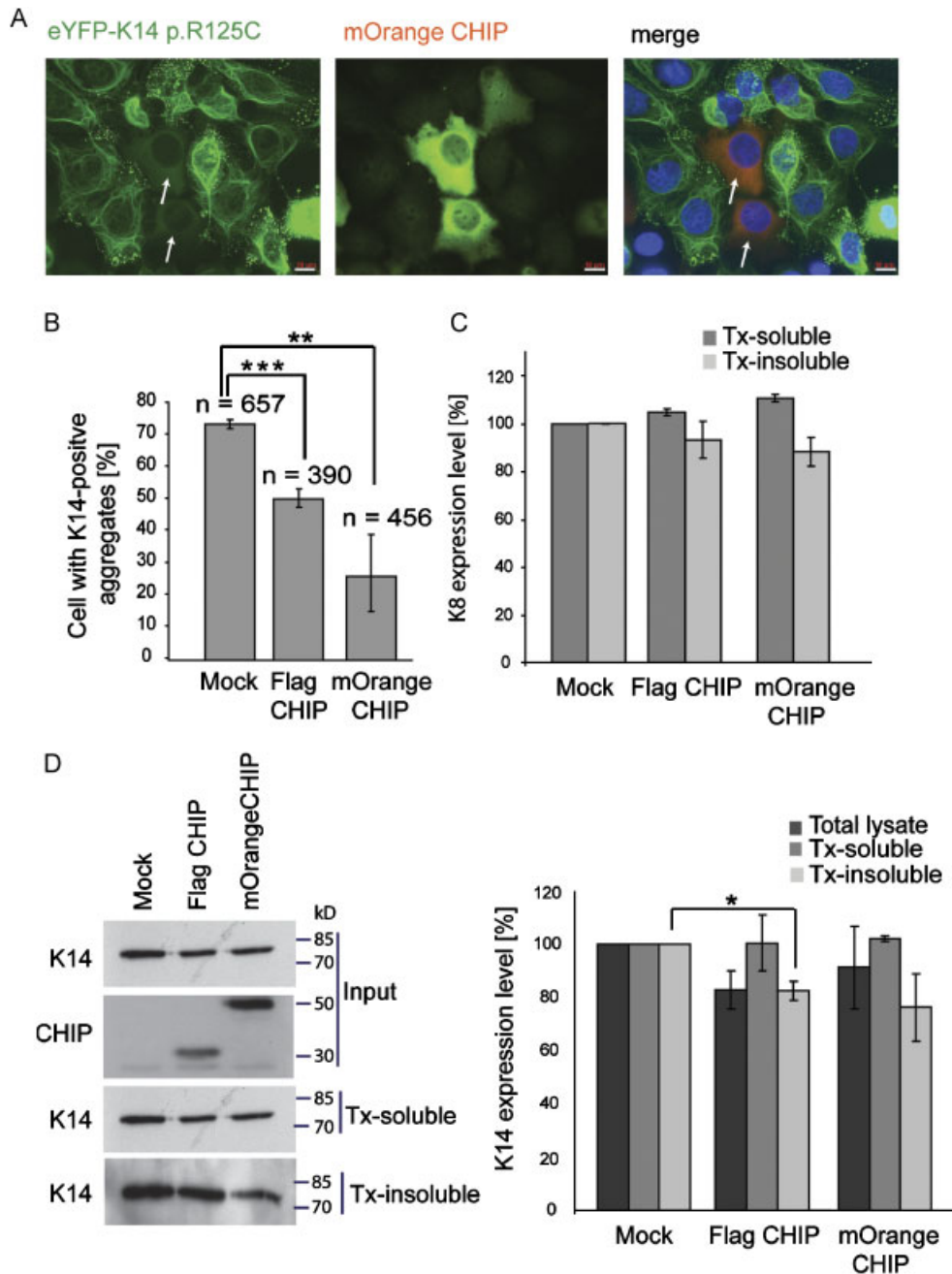


Figure 5. CHIP overexpression reduces K14-p.Arg125Cys-positive aggregates. Cells were transiently transfected with empty vector (mock) and either Flag-tagged or mOrange-tagged CHIP. After 24 hr, transfected cells were fixed and stained with DAPI. **A:** Autofluorescence of eYFP-K14-p.Arg125Cys (K14-p.R125C), mOrange CHIP, and merged images. Arrows indicate CHIP transfected cells and the absence of K14-p.Arg125Cys-positive aggregates in these cells compared to untransfected cells. Scale bar, 10 μ m. **B:** Quantification of total cells showing keratin 14-positive aggregates. $***P = 0.00005$; $**P = 0.0007$. **C:** Quantification of K8 from three different immunoblots of Triton X-100-soluble (Tx-soluble) and Triton X-100 insoluble (Tx-insoluble) fractions (immunoblots not shown). **D:** Left panel shows fractionation of cell lysates in Tx-soluble and Tx-insoluble fractions. Comparable amounts of protein were separated by 10% SDS-PAGE, transferred to nitrocellulose and immunoblotted with K14 and CHIP antibodies. Right panel shows quantification. $**P = 0.01$. Data are presented as means \pm SE of three independent experiments. The P values were calculated using the Student's t -test.

shares common principles with other protein misfolding disorders [Chamcheu et al., 2009; Lee et al., 2008]. Furthermore, we found that the expression of the severe mutation K14-p.Arg125Cys, which causes the loss of an intact keratin cytoskeleton and gives rise to extensive keratin aggregates, is targeted by the ubiquitin ligase CHIP. In line with this, high molecular weight species of the mutant K14, representing poly-ubiquitinated keratin, as well as a

colocalization of keratin aggregates and ubiquitin, were detected. The notion that overexpression of the E3 ligase CHIP promoted the proteasome-dependent degradation of keratins strongly suggests additional pathomechanisms in EBS and offers a novel route for therapy approaches.

Ubiquitination of keratins has been linked to an increase in serine phosphorylation [Ku and Omary, 2000]; however, whether

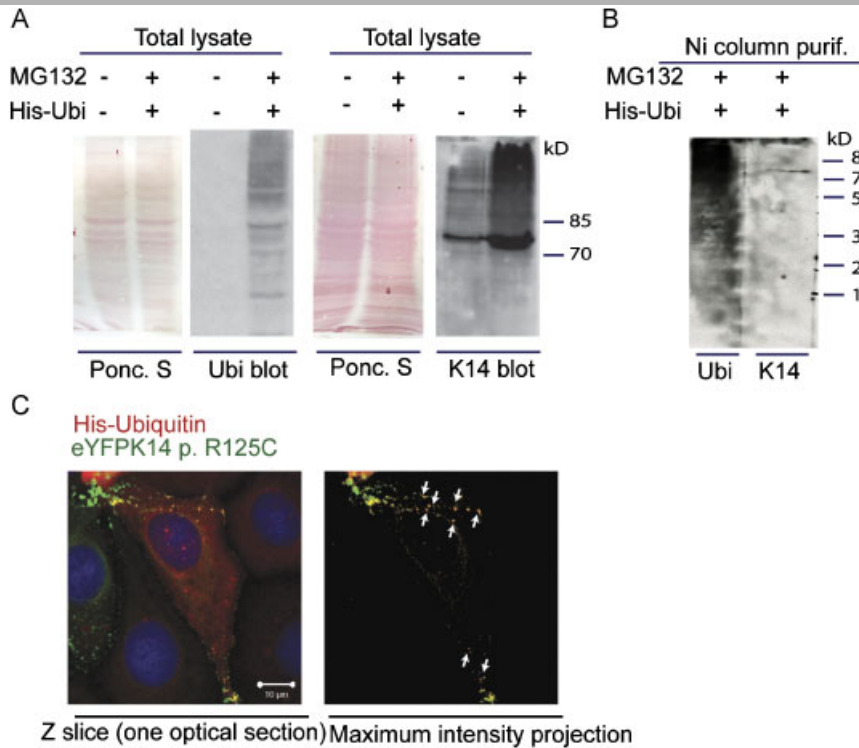


Figure 6. Mutant K14 is ubiquitinated in vivo. Cells, transiently transfected with empty vector and His-tagged ubiquitin were cultured in the absence or presence of MG132 (100 μ M) for 6 hr. **A:** Total cell lysates were prepared and equal amounts (Ponceaus S staining) were separated by 10% SDS-PAGE, transferred to nitrocellulose and immunoblotted with ubiquitin (left panel) and K14 (right panel) antibodies. **B:** Cells were solubilized and extracts were applied to a Ni-TED/IDA column. Purified His-tagged protein was separated by 15% SDS-PAGE and reacted with ubiquitin and K14 antibodies. **C:** His-ubiquitin transfectants stably expressing eYFP-K14-p.Arg125Cys (K14-p.R125C) were grown on cover slips, fixed, and stained with DAPI and anti-His(6) antibodies. Note colocalization of eYFP-K14-p.Arg125Cys (K14-p.R125C) with ubiquitin in the maximum intensity projection of colocalized pixels (right image, arrow heads). Scale bar, 10 μ m.

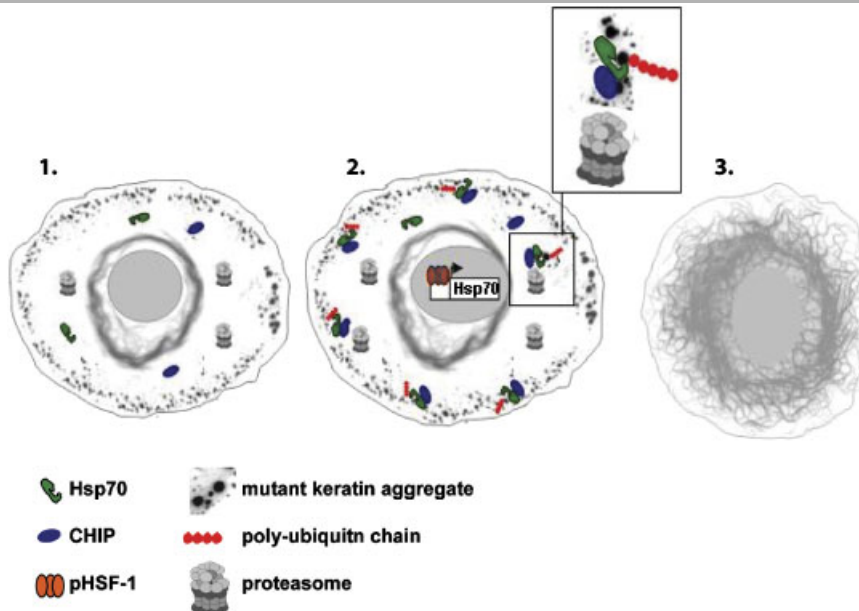


Figure 7. Proposed model of enhanced proteasomal degradation of mutant keratins. **1.** K14-p.Arg125Cys expressing cells with clusters of keratin aggregates in the cell periphery as well as remaining perinuclear keratin filaments. Expression levels of heat shock proteins are low. **2.** Induced Hsp70/CHIP complex formation (either by the experimental overexpression of CHIP or by an increase in nuclear translocation of the transcription factor pHSF-1, which can be experimentally induced), leads to the covalent coupling of polyubiquitin chains on Lys-residues in mutant keratins. This process may target preferentially the mutant keratin for proteasomal degradation. The inset shows a detailed view of the complex composed of Hsp70, CHIP and polyubiquitinated mutant keratin. **3.** The removal of mutant keratin aggregates in EBS patients will allow the formation of a normal keratin cytoskeleton from the intact keratin allele.

phosphorylation of keratins occurs in aggregates and is a prerequisite for CHIP-mediated ubiquitination, is not known at present. An alternative model is that certain mutations, including K14-p.Arg125Cys, cause protein misfolding, which by itself would be sufficient for CHIP recognition. The dispersal of insoluble, aggregated keratins requires the cooperation of a functional Hsc/p70-CHIP complex as demonstrated here by genetic and pharmacological inhibition of complex formation and Hsc/p70 inhibition, respectively. Confocal microscopy demonstrated a colocalization between K14 and the endogenous Hsc/p70 in MCF-7 cells. Furthermore, biochemical and genetical analysis data have shown the interaction of K5 as well as the K14 head domain with Hsc/p70. This suggests that this interaction might function as a scaffold to recruit its cochaperone CHIP. Future work will have to analyze whether mutant keratins are preferentially recognized by the Hsc/p70/CHIP complex.

The great majority of disease-causing *KRT5* and *KRT14* mutations initiate the transformation of a normal keratin cytoskeleton into cytosolic aggregates and render the epidermis susceptible following minor trauma. Until recently, it was widely believed that EBS pathology results merely from the absence of an intact cytoskeleton, despite increasing evidence for regulatory functions of keratins [Kim and Coulombe, 2007; Magin et al., 2007]. Recently, we found that genes encoding pro-inflammatory cytokines and chemokines that recruit Langerhans cells are upregulated in a mouse model for EBS and in patients [Roth et al., 2009]. Additionally, we reported an improved condition of an EBS mouse model by repressing pro-inflammatory and inducing wound repair-associated genes, following systemic application of doxycycline, a small molecule with anti-inflammatory properties [Lu et al., 2007]. In line with this, treatment of K14 knockout mice with sulphoraphane, a small molecule with anti-inflammatory properties, enhanced the survival of these mice, implicating that EBS patients with certain *KRT14* mutation may be successfully treated with this agent [Kerns et al., 2007]. In addition to these studies, which have revealed novel disease mechanisms, our current data support the view that chaperones and cochaperones play a role in EBS pathology.

Chaperones and cochaperones contribute to the pathology of protein misfolding disorders, and modulating their expression has been shown to affect protein misfolding and disease pathology, at least in model systems. This was reported first in models for PD and cystic fibrosis. Although in the first case a phenotypic reversion of cell toxicity in a *Drosophila* model for PD by elevating Hsp70 levels was reported [Auluck and Bonini, 2002; Auluck et al., 2002], the inhibition of Hsp70 prevented proteasome-dependent degradation of the $\Delta F508$ mutant of the cystic fibrosis transmembrane conductance regulator (CFTR) in a second model [Wang et al., 2007; Ward et al., 1995]. Given the clinical importance of protein misfolding disorders, a number of chemical and pharmacological chaperones and small molecules have been described to moderate chaperone activity at several levels, including HSF-1 modulators, as well as Hsp70 and Hsp90 inhibitors. Some of those inhibitors, for example geldanamycin, are already successfully used in the therapy of different forms of cancer [Moser et al., 2009].

In vivo studies have linked CHIP to AD and PD, suggesting a prominent role of this chaperone-associated ubiquitin ligase in protein quality control. Here, we show that the K14-p.Arg125Cys mutation renders it an excellent CHIP substrate that is recognized by a functionally Hsc/p70-CHIP complex, eventually leading to the proteasomal degradation of the mutant keratin. Other data support the preferential degradation of the mutant keratin,

because only K14-p.Arg125Cys, but not wild-type K14, was ubiquitinated in HaCaT cells [Yoneda et al., 2004]. Furthermore, ubiquitination and increased chaperone expression is a hallmark accompanying cataracts in mice and in humans carrying dominant-negative mutations in vimentin [Bornheim et al., 2008; Muller et al., 2009].

Our data have shown that aggregation-prone keratins are subjected to chaperone-assisted degradation (see model in Fig. 7). This implicates that elevated levels of the Hsc/p70-CHIP complex by small molecules should lead to the preferential degradation of mutant keratins and the removal of keratin aggregates. Given the dominant inheritance of severe EBS, this should allow formation of a normal keratin cytoskeleton from the intact allele. This is strongly supported by a mouse model in which overexpression of normal keratins caused normalization of tissue pathology caused by mutant keratins [Hesse et al., 2007]. Therefore, targeting chaperones and/or cochaperones might provide novel therapy approaches for EBS.

Acknowledgments

We thank Dr. W. Roth for kindly providing us back skin samples from K5-deficient mice. We are grateful to Dr. Cam Patterson (University of North Carolina at Chapel Hill, NC) for CHIP expression plasmids. We also thank Prof. Noegel, University of Cologne, for supplying GFP antibody. This work was partially funded by the DFG (MA1316-11), the BMBF (Netzwerk EB), the Bonner Forum Biomedizin, and the German Federal Ministry for Education and Research (BMBF) "Network epidermolysis bullosa" projects 6 (to L.B.-T.).

References

- Arndt V, Rogon C, Hohfeld J. 2007. To be, or not to be—molecular chaperones in protein degradation. *Cell Mol Life Sci* 64:2525–2541.
- Auluck PK, Bonini NM. 2002. Pharmacological prevention of Parkinson disease in *Drosophila*. *Nat Med* 8:1185–1186.
- Auluck PK, Chan HY, Trojanowski JQ, Lee VM, Bonini NM. 2002. Chaperone suppression of alpha-synuclein toxicity in a *Drosophila* model for Parkinson's disease. *Science* 295:865–868.
- Ballinger CA, Connell P, Wu Y, Hu Z, Thompson LJ, Yin LY, Patterson C. 1999. Identification of CHIP, a novel tetratricopeptide repeat-containing protein that interacts with heat shock proteins and negatively regulates chaperone functions. *Mol Cell Biol* 19:4535–4545.
- Bornheim R, Muller M, Reuter U, Herrmann H, Bussow H, Magin TM. 2008. A dominant vimentin mutant upregulates Hsp70 and the activity of the ubiquitin-proteasome system, and causes posterior cataracts in transgenic mice. *J Cell Sci* 121(Pt 22):3737–3746.
- Chamcheu JC, Lorie EP, Akgul B, Bannbers E, Virtanen M, Gammon L, Moustakas A, Navsaria H, Vahlquist A, Torma H. 2009. Characterization of immortalized human epidermolysis bullosa simplex (KRT5) cell lines: trimethylamine N-oxide protects the keratin cytoskeleton against disruptive stress condition. *J Dermatol Sci* 53:198–206.
- Coulombe PA, Kerns ML, Fuchs E. 2009. Epidermolysis bullosa simplex: a paradigm for disorders of tissue fragility. *J Clin Invest* 119:1784–1793.
- Dai Q, Zhang C, Wu Y, McDonough H, Whaley RA, Godfrey V, Li HH, Madamanchi N, Xu W, Neckers L, Cyr D, Patterson C. 2003. CHIP activates HSF1 and confers protection against apoptosis and cellular stress. *EMBO J* 22:5446–5458.
- Esser C, Alberti S, Hohfeld J. 2004. Cooperation of molecular chaperones with the ubiquitin/proteasome system. *Biochim Biophys Acta* 1695:171–188.
- Fine JD, Eady RA, Bauer EA, Bauer JW, Bruckner-Tuderman L, Heagerty A, Hintner H, Hovnanian A, Jonkman ME, Leigh I, McGrath JA, Mellerio JE, Murrell DF, Shimizu H, Uitto J, Vahlquist A, Woodley D, Zambruno G. 2008. The classification of inherited epidermolysis bullosa (EB): Report of the Third International Consensus Meeting on Diagnosis and Classification of EB. *J Am Acad Dermatol* 58:931–950.
- Fuchs E, Cleveland DW. 1998. A structural scaffolding of intermediate filaments in health and disease. *Science* 279:514–519.
- Helfand BT, Chang L, Goldman RD. 2004. Intermediate filaments are dynamic and motile elements of cellular architecture. *J Cell Sci* 117(Pt 2):133–141.
- Hesse M, Grund C, Herrmann H, Brohl D, Franz T, Omary MB, Magin TM. 2007. A mutation of keratin 18 within the coil 1A consensus motif causes widespread

- keratin aggregation but cell type-restricted lethality in mice. *Exp Cell Res* 313:3127–3140.
- Jaitovich A, Mehta S, Na N, Ciechanover A, Goldman RD, Ridge KM. 2008. Ubiquitin-proteasome-mediated degradation of keratin intermediate filaments in mechanically stimulated A549 cells. *J Biol Chem* 283:25348–25355.
- Kerns ML, DePianto D, Dinkova-Kostova AT, Talalay P, Coulombe PA. 2007. Reprogramming of keratin biosynthesis by sulforaphane restores skin integrity in epidermolysis bullosa simplex. *Proc Natl Acad Sci USA* 104:14460–14465.
- Kim S, Coulombe PA. 2007. Intermediate filament scaffolds fulfill mechanical, organizational, and signaling functions in the cytoplasm. *Genes Dev* 21:1581–1597.
- Kitajima Y, Inoue S, Yaoita H. 1989. Abnormal organization of keratin intermediate filaments in cultured keratinocytes of epidermolysis bullosa simplex. *Arch Dermatol Res* 281:5–10.
- Konig A, Lauharanta J, Bruckner-Tuderman L. 1992. Keratinocytes and fibroblasts from a patient with mutilating dystrophic epidermolysis bullosa synthesize drastically reduced amounts of collagen VII: lack of effect of transforming growth factor-beta. *J Invest Dermatol* 99:808–812.
- Ku NO, Omary MB. 2000. Keratins turn over by ubiquitination in a phosphorylation-modulated fashion. *J Cell Biol* 149:547–552.
- Lee D, Santos D, Al-Rawi H, McNeill AM, Rugg EL. 2008. The chemical chaperone trimethylamine N-oxide ameliorates the effects of mutant keratins in cultured cells. *Br J Dermatol* 159:252–255.
- Liovic M, Mogensen MM, Prescott AR, Lane EB. 2003. Observation of keratin particles showing fast bidirectional movement colocalized with microtubules. *J Cell Sci* 116(Pt 8):1417–1427.
- Lu H, Chen J, Planko L, Zigrino P, Klein-Hitpass L, Magin TM. 2007. Induction of inflammatory cytokines by a keratin mutation and their repression by a small molecule in a mouse model for EBS. *J Invest Dermatol* 127:2781–2789.
- Magin TM, Vijayaraj P, Leube RE. 2007. Structural and regulatory functions of keratins. *Exp Cell Res* 313:2021–2032.
- McClellan AJ, Scott MD, Frydman J. 2005. Folding and quality control of the VHL tumor suppressor proceed through distinct chaperone pathways. *Cell* 121:739–748.
- Moser C, Lang SA, Stoeltzing O. 2009. Heat-shock protein 90 (Hsp90) as a molecular target for therapy of gastrointestinal cancer. *Anticancer Res* 29:2031–2042.
- Muchowski PJ, Wacker JL. 2005. Modulation of neurodegeneration by molecular chaperones. *Nat Rev Neurosci* 6:11–22.
- Muller M, Bhattacharya SS, Moore T, Prescott Q, Wedig T, Herrmann H, Magin TM. 2009. Dominant cataract formation in association with a vimentin assembly disrupting mutation. *Hum Mol Genet* 18:1052–1057.
- Omary MB, Coulombe PA, McLean WH. 2004. Intermediate filament proteins and their associated diseases. *N Engl J Med* 351:2087–2100.
- Peters B, Kirfel J, Bussow H, Vidal M, Magin TM. 2001. Complete cytolysis and neonatal lethality in keratin 5 knockout mice reveal its fundamental role in skin integrity and in epidermolysis bullosa simplex. *Mol Biol Cell* 12:1775–1789.
- Planko L, Bohse K, Hohfeld J, Betz RC, Hanneken S, Eigelshoven S, Kruse R, Nothen MM, Magin TM. 2007. Identification of a keratin-associated protein with a putative role in vesicle transport. *Eur J Cell Biol* 86:827–839.
- Rosser MF, Washburn E, Muchowski PJ, Patterson C, Cyr DM. 2007. Chaperone functions of the E3 ubiquitin ligase CHIP. *J Biol Chem* 282:22267–22277.
- Roth W, Reuter U, Wohlenberg C, Bruckner-Tuderman L, Magin TM. 2009. Cytokines as genetic modifiers in K5^{-/-} mice and in human epidermolysis bullosa simplex. *Hum Mutat* 30:832–841.
- Russell D, Andrews PD, James J, Lane EB. 2004. Mechanical stress induces profound remodelling of keratin filaments and cell junctions in epidermolysis bullosa simplex keratinocytes. *J Cell Sci* 117(Pt 22):5233–5243.
- Schulz JB. 2008. Update on the pathogenesis of Parkinson's disease. *J Neurol* 255(Suppl 5):3–7.
- Schweizer J, Bowden PE, Coulombe PA, Langbein L, Lane EB, Magin TM, Maltais L, Omary MB, Parry DA, Rogers MA and others. 2006. New consensus nomenclature for mammalian keratins. *J Cell Biol* 174:169–174.
- Strnad P, Tao GZ, So P, Lau K, Schilling J, Wei Y, Liao J, Omary MB. 2008. "Toxic memory" via chaperone modification is a potential mechanism for rapid Mallory-Denk body reinduction. *Hepatology* 48:931–942.
- Tetzlaff JE, Putcha P, Outeiro TF, Ivanov A, Berezovska O, Hyman BT, McLean PJ. 2008. CHIP targets toxic alpha-Synuclein oligomers for degradation. *J Biol Chem* 283:17962–17968.
- Wang Y, Loo TW, Bartlett MC, Clarke DM. 2007. Additive effect of multiple pharmacological chaperones on maturation of CFTR processing mutants. *Biochem J* 406:257–263.
- Ward CL, Omura S, Kopito RR. 1995. Degradation of CFTR by the ubiquitin-proteasome pathway. *Cell* 83:121–127.
- Watson ED, Geary-Joo C, Hughes M, Cross JC. 2007. The Mrj co-chaperone mediates keratin turnover and prevents the formation of toxic inclusion bodies in trophoblast cells of the placenta. *Development* 134:1809–1817.
- Werner NS, Windoffer R, Strnad P, Grund C, Leube RE, Magin TM. 2004. Epidermolysis bullosa simplex-type mutations alter the dynamics of the keratin cytoskeleton and reveal a contribution of actin to the transport of keratin subunits. *Mol Biol Cell* 15:990–1002.
- Windoffer R, Kolsch A, Woll S, Leube RE. 2006. Focal adhesions are hotspots for keratin filament precursor formation. *J Cell Biol* 173:341–348.
- Windoffer R, Leube RE. 2004. Imaging of keratin dynamics during the cell cycle and in response to phosphatase inhibition. *Methods Cell Biol* 78:321–352.
- Woll S, Windoffer R, Leube RE. 2005. Dissection of keratin dynamics: different contributions of the actin and microtubule systems. *Eur J Cell Biol* 84:311–328.
- Woll S, Windoffer R, Leube RE. 2007. p38 MAPK-dependent shaping of the keratin cytoskeleton in cultured cells. *J Cell Biol* 177:795–807.
- Yoneda K, Furukawa T, Zheng YJ, Momoi T, Izawa I, Inagaki M, Manabe M, Inagaki N. 2004. An autocrine/paracrine loop linking keratin 14 aggregates to tumor necrosis factor alpha-mediated cytotoxicity in a keratinocyte model of epidermolysis bullosa simplex. *J Biol Chem* 279:7296–7303.
- Zatloukal K, French SW, Stumptner C, Strnad P, Harada M, Toivola DM, Cadrin M, Omary MB. 2007. From Mallory to Mallory-Denk bodies: what, how and why? *Exp Cell Res* 313:2033–2049.
- Zhou Q, Toivola DM, Feng N, Greenberg HB, Franke WW, Omary MB. 2003. Keratin 20 helps maintain intermediate filament organization in intestinal epithelia. *Mol Biol Cell* 14:2959–2971.